# THIN ICE AREA EXTRACTION IN THE SEASONAL SEA ICE ZONES OF THE NORTHERN HEMISPHERE USING MODIS DATA

K. Hayashi [1], K. Naoki [1], K. Cho [1]*,

[1]Tokai University, 2-28-4, Tomigaya, Shibuya-ku, Tokyo, Japan, kohei.cho@tokai-u.jp

**Commission III, WG III/9**

**KEY WORDS:** Sea Ice, Optical Sensor, Global Warming, Glaciology

**ABSTRACT:**

Sea ice has an important role of reflecting the solar radiation back into space. However, once the sea ice area melts, the area starts to absorb the solar radiation which accelerates the global warming. This means that the trend of global warming is likely to be enhanced in sea ice areas. In this study, the authors have developed a method to extract thin ice area using reflectance data of MODIS onboard Terra and Aqua satellites of NASA. The reflectance of thin sea ice in the visible region is rather low. Moreover, since the surface of thin sea ice is likely to be wet, the reflectance of thin sea ice in the near infrared region is much lower than that of visible region. Considering these characteristics, the authors have developed a method to extract thin sea ice areas by using the reflectance data of MODIS (NASA MYD09 product, 2017) derived from MODIS L1B. By using the scatter plots of the reflectance of Band 1(620nm-670nm) and Band 2(841nm-876nm)) of MODIS, equations for extracting thin ice area were derived. By using those equations, most of the thin ice areas which could be recognized from MODIS images were well extracted in the seasonal sea ice zones in the Northern Hemisphere, namely the Sea of Okhotsk, the Bering Sea and the Gulf of Saint Lawrence. For some limited areas, Landsat-8 OLI images were also used for validation

## 1. INTRODUCTION

The time series observations by the passive microwave radiometers onboard satellites strongly suggest the large decadal decline trend of the Arctic sea ice cover (Comiso, 2012, JAXA, 2012, NSIDC, 2018 etc.). The trend of the sea ice cover reduction is referred as an evidence of global warming in the Fifth Assessment Report of IPCC (2014). The importance of sea ice monitoring from space is increasing. Under the cloud free condition, optical sensors onboard satellites allow us to monitor the detailed condition of sea ice with wide view. In monitoring sea ice, ice thickness is one of the important parameters. Various studies on estimating ice thickness with optical sensors onboard satellites have been performed in the past (Such as Allison, 1993, Perovich et al., 1982, and Grenfell, 1983). Cho et al. (2011, 2012) has done detailed studies on comparing the in situ ice thickness measurement result with the data observed by optical sensors such as RSI on FORMOSAT-2 and MODIS on Aqua/Terra. The result suggested that if the ice thickness is less than 20 to 30cm, the ice thickness difference can be detected with optical sensors such as RSI and MODIS. Since the heat flux of ice is strongly affected by the ice thickness (Maykut, 1978), extracting thin ice area is quite important. The authors have developed a method to extract thin ice area in the Sea of Okhotsk using data of MODIS onboard Terra and Aqua satellites (Hayashi et al, 2016). The main idea is to extract thin ice area which thickness is less than around 30cm using the scatter plots of MODIS reflectance data. Considering the spatial resolution of MODIS, the ice thickness estimation is not considered in this method. This time, the authors have applied the algorithm also to the other seasonal sea ice zones in the Northern Hemisphere i.e. the Sea of Bering and the Gulf of Saint Lawrence.

*Corresponding author: Kohei Cho, Tokai University Research & Information Center, 2-28-4, Tomigaya, Shibuya-ku, Tokyo151-0063, Japan

## 2. TEST SITE

The authors have selected the Sea of Okhotsk, the Bering sea and the Gulf of Saint Lawrence as the test sites in this study. Figure 1 show the map of the three test sites. The Sea of Okhotsk is located at the north side of Hokkaido, Japan, surrounded by the Island of Sakhalin and eastern Siberian coast, Kamchatka Peninsula and Kuril Islands. The sea is one of the most southern seasonal sea ice zones in the northern hemisphere, and many thin ice areas can be found in the sea. The Bering Sea is located in the northernmost part of the Pacific Ocean, which is surrounded by the Siberia, the Kamchatka Peninsula, the Alaska Peninsula and the Aleutian Islands. The Bering Sea is connected to Arctic Ocean by the Bering Strait. The Gulf of St. Lawrence is a kind of inland sea located in eastern Canada. It is the outlet of North America's Great Lakes via the Saint Lawrence River into the Atlantic Ocean.

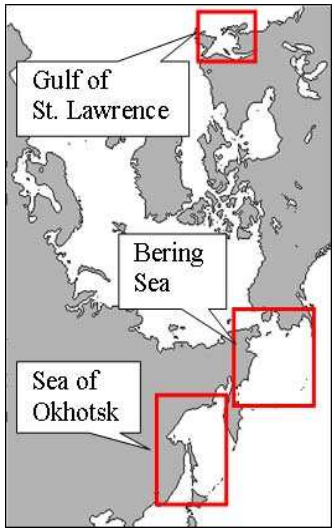


**Figure 1. Map of the test sites (NSIDC, 2010)**

This contribution has been peer-reviewed.
https://doi.org/10.5194/isprs-archives-XLII-3-485-2018 | © Authors 2018. CC BY 4.0 License.

## 3. ANALYZED DATA

For evaluating the possibility of extracting thin ice areas with optical sensors, MODIS data taken from on board Terra and Aqua satellites were analysed in this study. Actually, reflectance data (NASA MYD09 product, 2017) derived from MODIS L1B data were used in this study. Table 1 shows the specifications of MODIS. In order to utilize the highest spatial resolution of MODIS, we used only Band 1 and 2 which have 250m resolution. In order the evaluate the detailed distribution of thin ice, the optical sensor OLI images of Landsat-8 were used as references. Table 2 shows the specifications of OLI. Since the spatial resolution (IFOV) of OLI is much higher that of MODIS, one can identify much details of thin ice area with OLI images than MODIS images.

**Table.1 Specifications of optical sensor MODIS**

| Band | Wavelength | IFOV | Swath |
|---|---|---|---|
| 1 | 0.620 - 0.670μm | 250m | 2330km |
| 2 | 0.841 - 0.876μm | | |
| 3 -7 | 0.459 - 2.155μm | 500m | |
| 8 – 36 | 0.405 - 14.385μm | 1000m | |

(NASA, 2010)

**Table.2 Specifications of optical sensor OLI**

| Band | Wavelength | IFOV | Swath |
|---|---|---|---|
| 1 | 0.433-0.453μm | 30 m | 185km |
| 2 | 0.450-0.515μm | | |
| 3 | 0.525-0.600μm | | |
| 4 | 0.630-0.680μm | | |
| 5 | 0.845-0.885μm | | |
| 6 | 1.560-1.660μm | | |
| 7 | 2.100-2.300μm | | |
| 8 | 0.500-0.680μm | 15 m | |
| 9 | 1.360-1.390μm | 30 m | |

(USGS, 2014)

## 4. TEST AREA SELECTION

The reflectance of thin sea ice area is rather low in visible and near-infrared portion of the spectrum. Especially, the near-infrared portion of the spectrum is quite sensitive to water, and the reflectance dramatically reduces with the existence of water. Since the surface of thin sea ice is likely to be wet, usually the reflectance of near-infrared band (MODIS Band 2) is much lower than that of visible band (MODIS Band 1) in thin sea ice areas (Cho et al., 2012). Figure 2 shows a color composite image of MODIS assigning blue & red to band 1(visible) and green to band 2(near-infrared). Since the reflectance of ice reduces in band 2 when the ice is covered or surrounded by water, the thin ice areas are likely to appear in purple in the MODIS image. In order to investigate the possibility of extracting thin ice area using MODIS data, the authors have selected the test areas for thin ice, open water, cloud, and big ice floe from an MODIS image of the Sea of Okhotsk observed on February 23, 2014 as shown on Figure 2. The dark thin ice area (a) and light thi ice area(b) were selected along the coast of Russia. The cloud area (c) was selected over the open water near the Kamchatka Peninsula. The big ice floe area(d) was selected in the east side of Sakhalin and the open water area (e) was selected in the west side of Sakhalin.

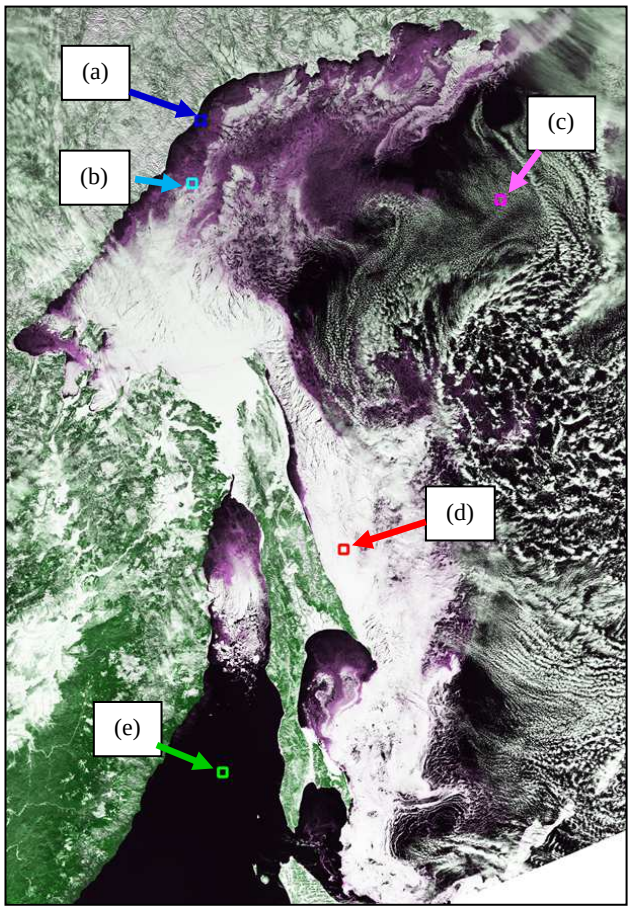


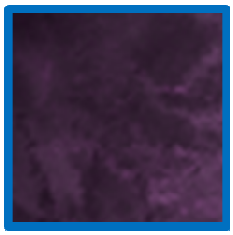

(a) Dark thin ice

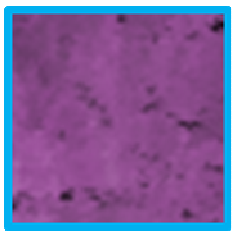

(c) Light thin ice

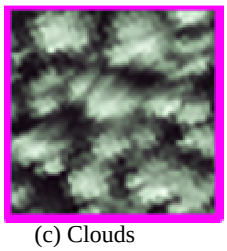

(c) Clouds

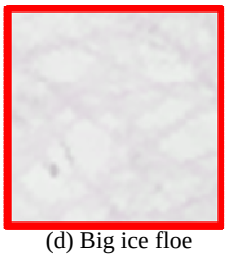

(d) Big ice floe

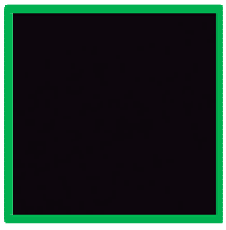

(e)Open Water

**Figure 2. Extraction of test area from the MODIS image.(Sea of Okhotsk, February 23, 2014)**

## 5. THIN ICE AREA EXTRACTION ALGORITHM

Figure 3 show the scatter plot of the four test items of big ice floe(■), thin ice(▲), cloud(◆), and open water(●) on the Band 1 VS Band 2 diagram. The gray dots(■) correspond to the hole distribution of the Sea of Okhotsk. In our previous study (Hayashi, 2016), the authors have used numerical value of MODIS L1B. However, since the distribution of each items in the scatter diagram were not stable from time to time, the authors have decided to use the reflectance derived from MODIS in this study. Considering the distribution of each item in Figure 3, the authors have derived the following three equations to extract the thin ice area.

$$B2<0.55\times B1+3 \quad (1)$$
$$B1<55 \quad (2)$$
$$B2<B1-2 \quad (3)$$

where B1: Reflectance of MODIS Band 1
B2: Reflectance of MODIS Band 2

By using the equation (1), (2) and (3), the pixels which are plotted in the red meshed area in Figure 4 will be classified to thin ice area in this algorithm.

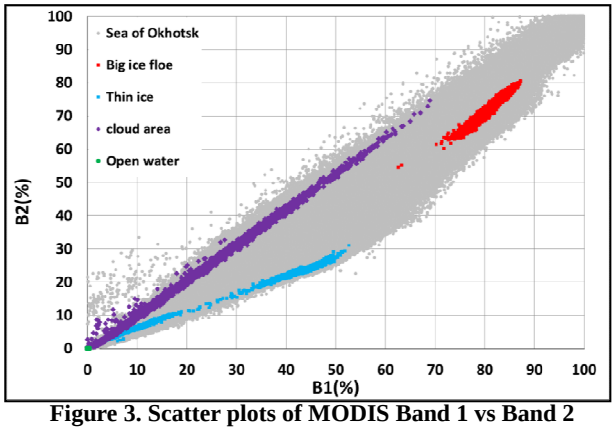


**Figure 3. Scatter plots of MODIS Band 1 vs Band 2 (Sea of Okhotsk, February 23, 2014)**

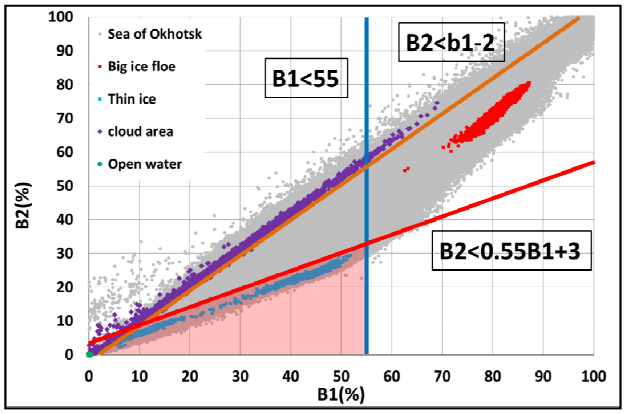


**Figure 4. Concept of thin ice area extraction using the scatter plot of MODIS Band 1 vs Band 2 (Sea of Okhotsk, February 23, 2014)**

## 6. EXTRACTED RESULT

The authors have applied this algorithm to the thee seasonal sea ice zones in the northern hemisphere which are the Sea of Okhotsk, the Bering Sea, and the Gulf of Saint Lawrence. The results are described in below.

### 6.1 Sea of Okhotsk

The MODIS data of the Sea of Okhotsk observed on February 23, 2014 was processed by using the equation (1) to (3) for thin ice area extraction. The extracted thin ice areas are overlaid on the MODIS image in light blue as shown on Figure 5. Most of the thin ice area appearing in dark purple in the MODIS image as sown on Figure 2 were well extracted with this algorithm. Especially, the discrimination of thin ice areas from clouds are very good as shown on Figure 5(c) and (d).

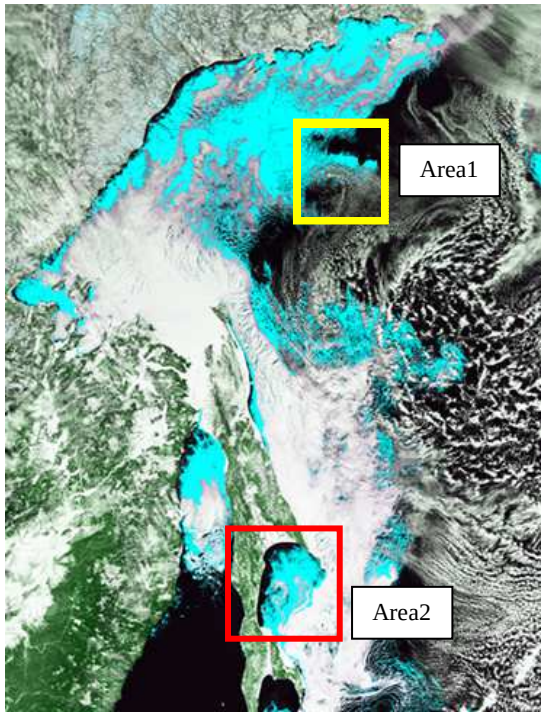


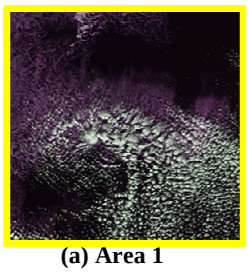

**(a) Area 1**

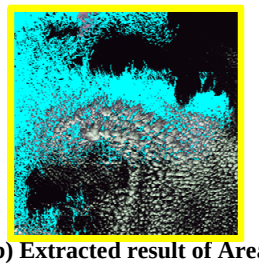

**(b) Extracted result of Area 1**

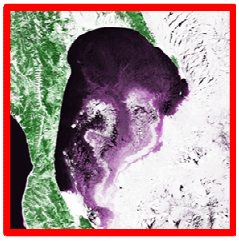

**(c) Area 2**

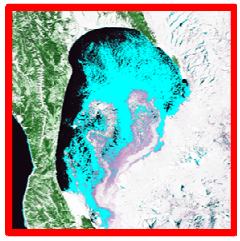

**(d) Extracted result of Area 2**

**Figure 5. Thin ice area extraction result (MODIS, Sea of Okhotsk, February 23, 2014)**

Figure 6 show another example of extracting test areas from the MODIS data of the Sea of Okhotsk observed on March 13, 2016. Figure 7 show the scatter plot of the four test items on the Band 1 VS Band 2 diagram. Figure 8 shows the result of thin ice area extraction.

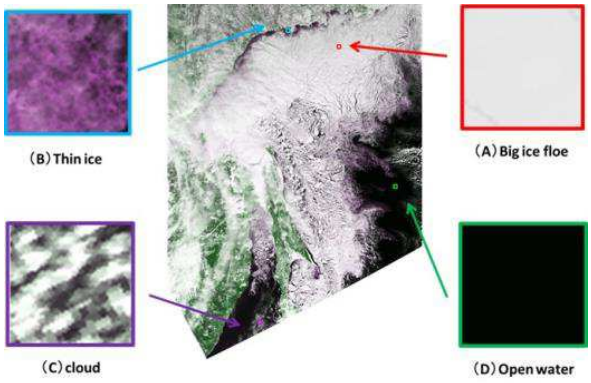


**Figure 6. Extraction of test area from the MODIS image.(Sea of Okhotsk, March 13, 2016)**

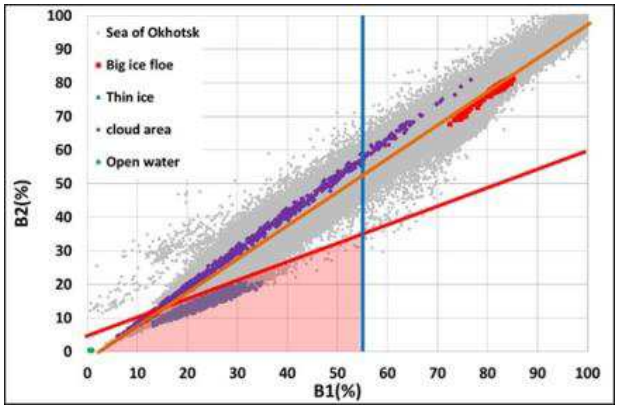


**Figure 7. The scatter plot of MODIS Band 1 vs Band 2 used for extracting thin ice areas for the Sea of Okhotsk on March 13, 2016.**

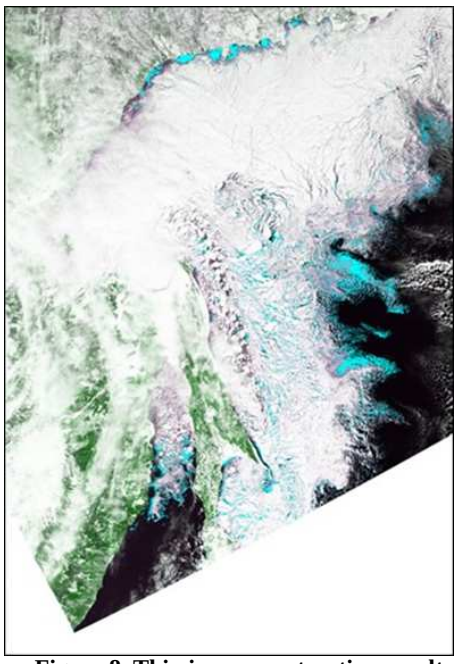

**Figure 8. Thin ice area extraction result (MODIS, Sea of Okhotsk, February 23, 2014)**

### 6.2 Bering Sea

The algorithm was also applied to the MODIS data of the Bering Sea. The results are shown on Figure 9. Most of the thin ice areas which can be visually recognized in the MODIS images were well extracted with this method without changing the parameters of equation (1) to (3).

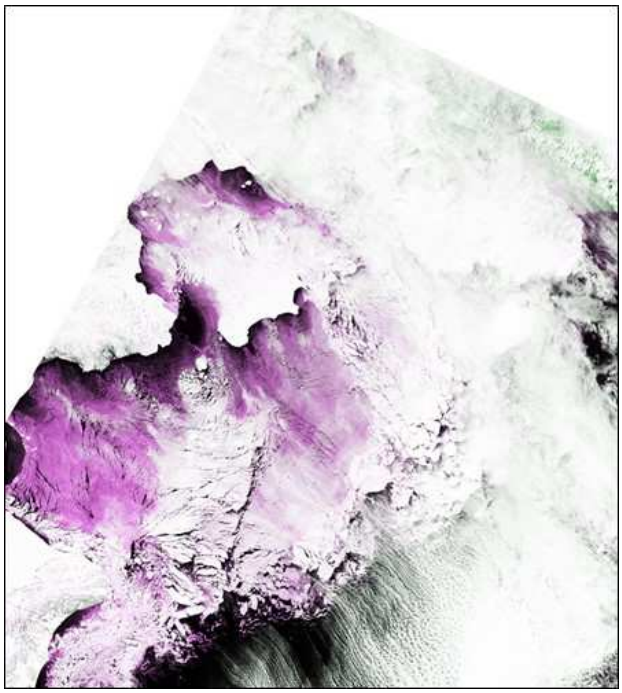

(a) MODIS image

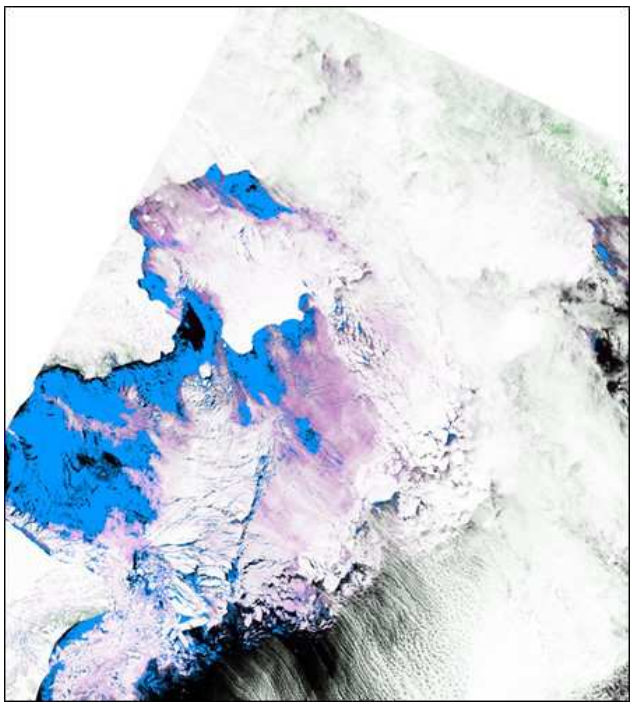

(b) Extracted result

**Figure 9. Thin ice area extraction result from MODIS image.**
**(Bering Sea, February 10, 2015)**

### 6.3 Gulf of Saint Lawrence

Figure 10 show the thin ice area extraction result of the Gulf of Saint Lawrence from MODIS data observed on March 13, 2015, and Figure 11 show the thin ice area extraction result of the Gulf of Saint Lawrence from MODIS data observed on March 8, 2016,.

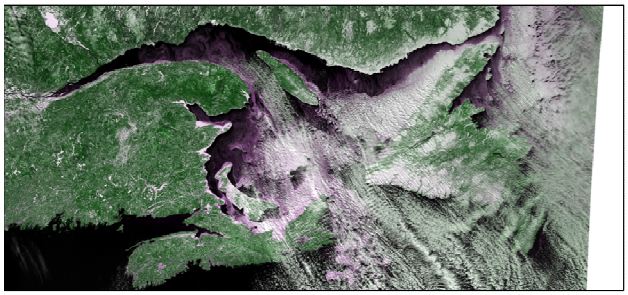

(a) MODIS image

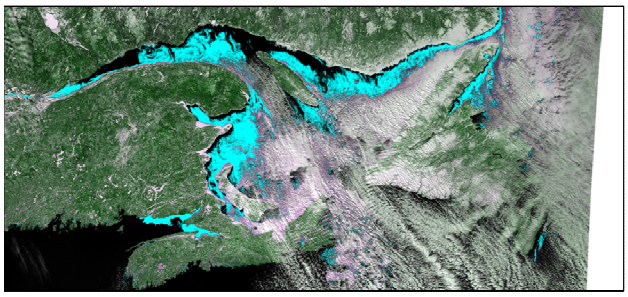

(b) Extracted result

**Figure 10. Thin ice area extraction result from MODIS image. (Gulf of Saint Lawrence, March 13, 2015)**

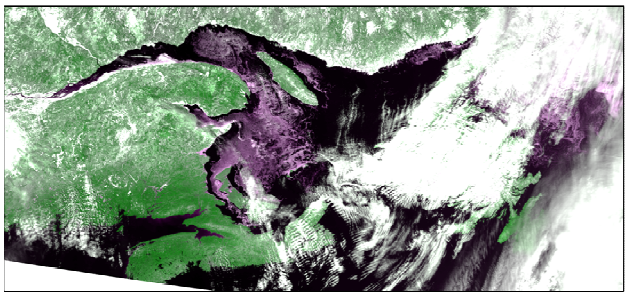

(a) MODIS image

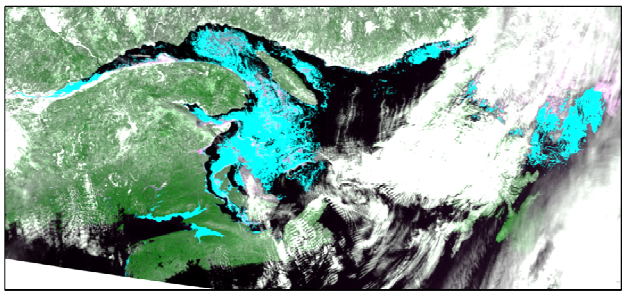

(b) Extracted result

**Figure 11. Thin ice area extraction result from MODIS image. (Gulf of Saint Lawrence, March 8, 2016)**

## 7. COMPARISON WITH OLI IMAGES

The thin ice area extracted from MODIS data were compared with OLI images of Landsat-8 observed on the same day in the Sea of Okhotsk and in the Bering Sea. Since the spatial resolution (IFOV) of OLI images are much higher than that of MODIS, much details of thin ice area distribution can be observed with OLI images. Considering the one scene size of OLI, only a part of each MODIS images was compared with OLI image.

### 7.1 Sea of Okhotsk

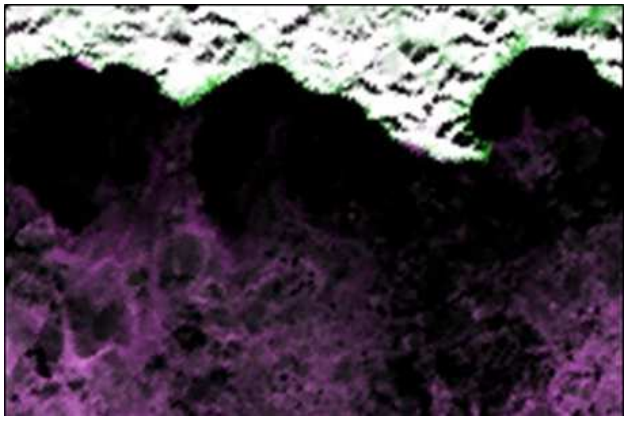

(a) MODIS image

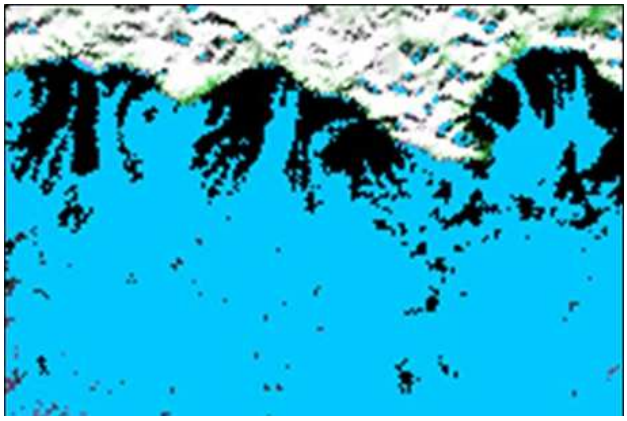

(b) Extracted result

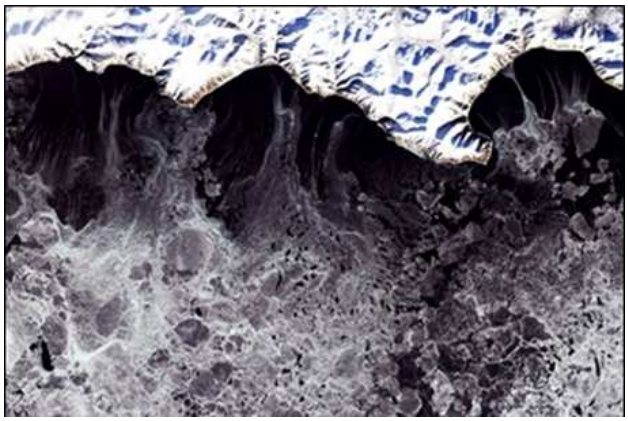

**(c) OLI image**

**Figure 12. Comparison of thin ice area extraction result from MODIS image with LOI image.**

**(Sea of Okhotsk, February 28, 2016)**

### 7.2 Bering Sea

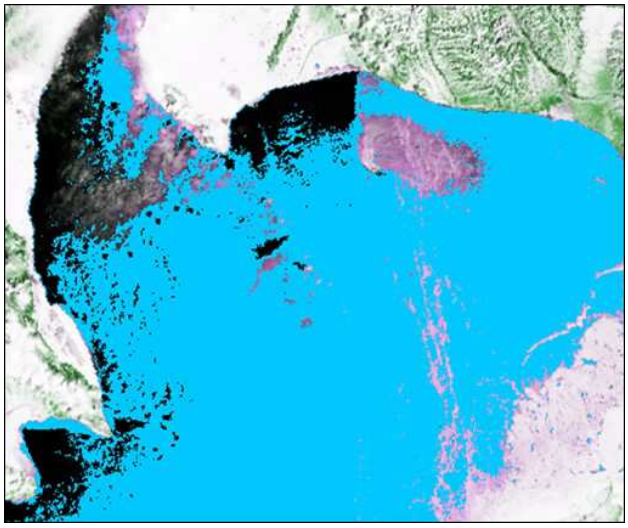

(a) Extracted thin ice areas overlaid on MODIS image

**(c) OLI image**

**Figure 13. Comparison of thin ice area extraction result from MODIS image with LOI image.**
**(Bering Sea, March 21, 2016)**

## 8. CONCLUSION

In this study, the authors have developed a method to extract thin sea ice areas by using the scatter plots of reflectance derived from MODIS Band 1 and 2 data. By applying the three equations to the MODIS Band 1&2 domain, most of the thin ice areas which were visually recognized in the MODIS images were well extracted not only in the Sea of Okhotsk, but also in the Bering Sea and in the Gulf of Saint Lawrence. The comparison of the extracted results with high resolution OLI images of Landsat 8 suggested the reliability of the method. The discrimination of thin ice areas from clouds were also reasonable. However, some thin clouds over open water were likely to be extracted as thin ice area with this algorithm. The authors are now working to solving this problem.

## ACKNOWLEDGEMENT

This study was partly supported by JAXA under the frame work of GCOM-W Verification Program. The authors would like to thank JAXA on their kind support.

## REFERENCES

Comiso, J., 2012, Large Decadal Decline of the Arctic Multiyear Ice Cover, Journal of Climate, Vol. 25, pp.1176-1193.

JAXA, 2012, Arctic Sea Ice Observation Data Analysis Results, Press Release, http://global.jaxa.jp/press/2012/08/20120825_arctic_sea_e.html.

NSIDC, 2018, Arctic sea ice maximum at second lowest in the satellite record, http://nsidc.org/arcticseaicenews/

IPCC. 2014. “Summary for Policymakers.” In Climate Change 2013: The Physical Basis. Contribution of Working Group I to the Fifth Assessment Report of the Intergovernmental Panel on Climate Change, edited by T.F. Stocker, D. Qin, G.K. Plattner, *et al*., Cambridge: Cambridge University Press.

Allison, I., 1993, East Antarctic sea ice: albedo, thickness distribution, and snow cover”, J. Geophys. Res., Vol. 98, pp.12417-12429.

Perovich , D. K. and T. C. Grenfell, 1982, “A theoretical model of radiative transfer in young sea ice”, J. Glaciol., Vol.28, pp. 341-356.

T. C. Grenfell, 1983, “A theoretical model of the optical properties of sea ice in the visible and near infrared”, J. Geophys. Res., 88, 9723-9735.

Cho, K., Y. Mochiduki, Y. Yoshida, M. Nakayama, K. Naoki, C.F. CHEN, 2011, Thin ice thickness monitoring with FORMOSAT-2 RSI data, Proceedings of the 32nd Asian Conference on Remote Sensing, TS1-2, pp.1-8.

Cho, K., Y. Mochizuki, Y. Yoshida, H. Shimoda and C.F. CHEN, 2012, A study on extracting thin sea ice area from space, International Archives of the Photogrammetry, Remote Sensing and Spatial Information Sciences, Vol. XXXIX-B8, pp.561-566.

Martin, S., R. Drucker, R. Kwok, and B. Holt, 2004, Estimation of the thin ice thickness and heat flux for the Chukchi Sea Alaskan coast polynya from Special Sensor Microwave/Imager data, 1990–2001. *J. Geophys. Res.*, *Vol.*109, C10012,

Maykut, G. A., 1978, Energy exchange over young sea ice in the central arctic, JGR, Vol.83, pp.3646-3658.

Hayashi, K., K. Naoki, K. Cho, 2016, Extraction of Thin Ice Area in the Sea of Okhotsk, Proceedings of the 37th Asian Conference on Remote Sensing, Ab 0559, pp.1-5.

NSIDC, 2010, http://nsidc.org/data/

NASA, 2017, MYD09, https://ladsweb.modaps.eosdis.nasa.gov/api/v1/productPage/product=MYD09

NASA, 2010, http://modis.gsfc.nasa.gov/

USGS, 2014, https://landsat.usgs.gov/landsat-8-l8-data-users-handbook